

In Situ Nano-thermo-mechanical Experiment Reveals Brittle to Ductile Transition in Si Nanowires

Guangming Cheng¹ and Yong Zhu²

¹Princeton University, Princeton, New Jersey, United States, ²North Carolina State University, Raleigh, North Carolina, United States

Silicon nanostructures have been used extensively in modern microelectronics. The ever-increasing integration density in microelectronic chips inevitably leads to a marked temperature rise of Si nanostructures, which are required to withstand large thermal stresses for maintaining their proper functions. Si nanostructures are also the building blocks for many novel nanotechnology applications, including energy harvesting and storage, flexible and stretchable electronics, sensors and nanoelectromechanical systems.[1] The reliability concerns of these applications call for a fundamental understanding of the mechanical behavior of Si nanostructures at elevated temperatures. Here we report the *in situ* tensile testing of single crystal Si NWs in the temperature range of RT to 600 K.[2] We employ a newly developed microelectromechanical system (MEMS)[3-6] for conducting the nano-thermo-mechanical testing inside a transmission electron microscope (TEM). This platform allows stress-strain measurement with simultaneous TEM imaging of atomic-scale deformation at different temperatures.[2,7] An on-chip heater is built into the MEMS-based platform, allowing the controlled heating of the specimen.

Single crystal Si NWs were synthesized by chemical evaporation deposition through the vapor-liquid-solid mechanism. The Si NWs used for mechanical testing are $\langle 112 \rangle$ -oriented and have a central $\{111\}$ twin boundary running parallel to the axial direction of the NW. *In situ* TEM tensile testing of individual Si NWs was performed at temperatures ranging from 295 to 600 K. Fig. 1 reveals that the Si NWs under tension are brittle at RT, but exhibit pronounced plastic deformation followed by fracture at elevated temperatures (e.g., 600 K). Fig. 1a shows the stress-strain curve of a Si NW with a diameter of 61 nm at 295 K. This NW initially exhibited a linear elastic response. As the tensile strain increased to 7.4% and the corresponding tensile stress to 11.5 GPa, brittle fracture occurred. As shown in Fig. 1b, the tensile stress-strain curve was initially linear and became slightly nonlinear with increasing stress, until the maximum stress of 5.8 GPa was reached at the critical strain of 4.0%. Subsequently, the stress decreased with increasing strain, and this softening response continued until fracture occurred at the strain of 4.7%. The inset in Fig. 1b shows the TEM image of fracture surfaces, which exhibit the features of ductile failure such as localized necking, deformation bands and rough fracture planes. Figure 1c shows the TEM snapshots during *in situ* tensile testing at 600 K, and the corresponding stress/strain for each snapshot is marked in Fig. 1b. It is seen that the maximum stress and ensuing softening response can be associated with surface nucleation and migration of dislocations as well as dislocation interactions with the twin boundary, as marked by blue arrows in Fig. 1c *ii-iv*. These continued dislocation processes resulted in large plastic strains in Si NWs at elevated temperatures. We also found that a decrease in the NW diameter can lead to enhanced plastic deformation. Fig. 1b includes the tensile stress-strain curve of a thinner Si NW with a diameter of 24 nm at 600 K, which is qualitatively similar to the Si NW with a diameter of 66 nm at 600 K. However, in this thinner NW, a lower maximum stress of 5.1 GPa was attained at a smaller critical strain of 4.3%, signifying a stronger tendency to plastic deformation. Moreover, the subsequent softening response was sustained over a strain range of 1.6% until the fracture strain ϵ_f of 5.9%; this strain range is defined as plastic strain ϵ_p . Hence, both ϵ_p and ϵ_f measured for the thinner Si NW are larger than the corresponding ϵ_p of 0.7% and ϵ_f of 4.7% for the thicker Si NW (Fig. 1b). The more extensive plasticity

in the thinner Si NW was manifested by the formation of a number of deformation bands that are uniformly distributed throughout the entire NW, which contrasts with fewer deformation bands in the thicker NW (Fig. 1c).

To further understand the size and temperature dependence of dislocation-mediated plasticity and fracture, we tested 78 Si NWs with the diameter range of 24–160 nm and in the temperature range of 295–600 K. As shown in Fig. 2a, the plastic strain ϵ_p increases with decreasing NW diameter. For example, at 600 K, ϵ_p increases from 0.27 to 1.6%, as the NW diameter decreases from 160 to 24 nm. For the same diameter, ϵ_p increases with temperature. The results of the 78 Si NWs tested are summarized in a deformation mechanism map of Fig. 2b. In this map, green circles represent Si NWs with dislocation-mediated failure, while black squares Si NWs with brittle cleavage fracture. A transition line, as defined by a critical ϵ_p of 0.1%, is drawn to separate the regimes of brittle and dislocation-mediated responses. The map also reveals that as the NW diameter decreases, the critical temperature associated with dislocation-mediated plastic deformation decreases. For example, the Si NW with diameter of 110 nm showed brittle fracture at 398 K, while the NW with diameter of 30 nm exhibited plastic deformation with dislocation activities even at 362 K. Hence, Fig. 2b indicates that both the increase of temperature and the decrease of NW diameter can promote plastic deformation in Si NWs, leading to dislocation-mediated failure.[8]

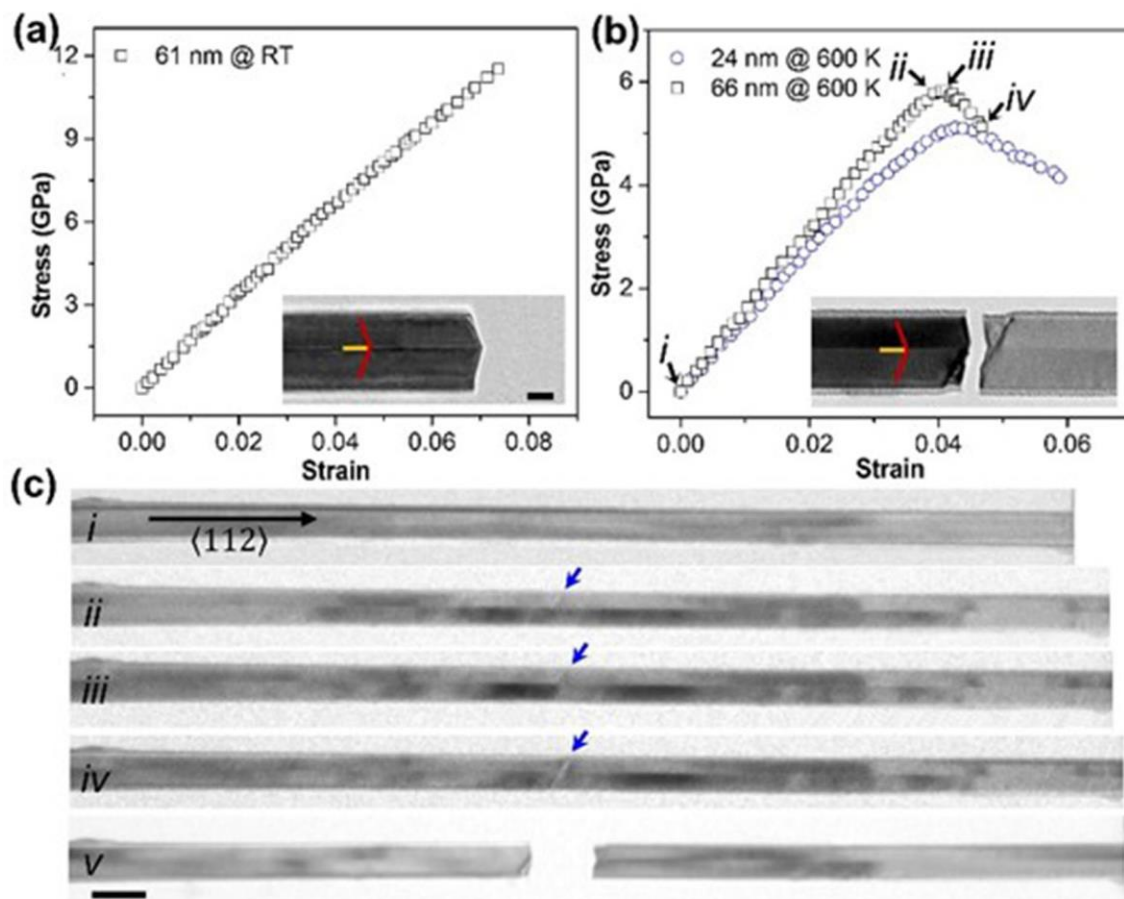


Figure 1. In situ MEMS-based measurement and TEM observation of mechanical behavior of individual Si NWs under uniaxial tension at room and elevated temperatures.

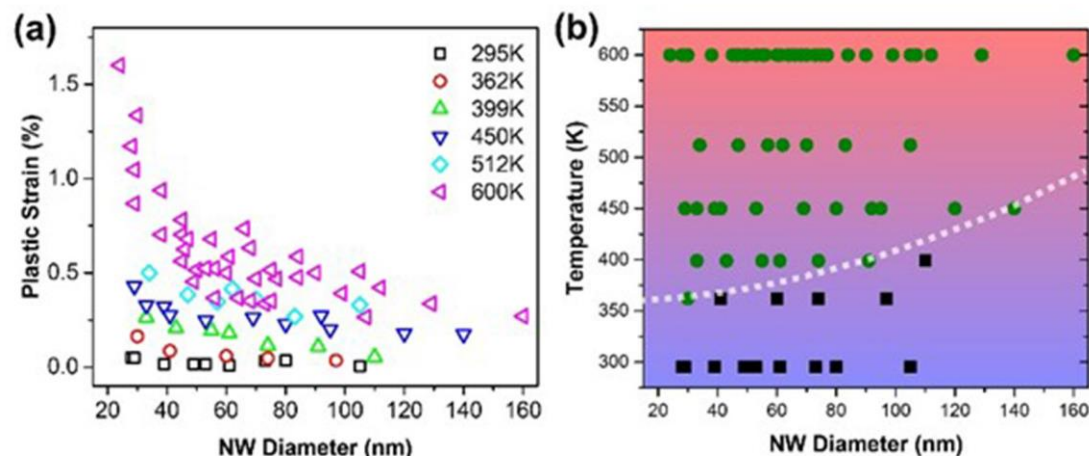


Figure 2. Size and temperature dependence of brittle versus ductile behaviors of 78 Si NWs tested in the temperature range of 295 to 600 K.

References

- [1] F. Xu, W. Lu, and Y. Zhu, *Acs Nano* **5**, 672 (2011).
- [2] G. Cheng, Y. Zhang, T.-H. Chang, Q. Liu, L. Chen, W. D. Lu, T. Zhu, and Y. Zhu, *Nano Letters* **19**, 5327 (2019).
- [3] G. M. Cheng, S. Yin, T. H. Chang, G. Richter, H. J. Gao, and Y. Zhu, *Physical Review Letters* **19**, 256101, 256101 (2017).
- [4] S. Yin, G. Cheng, G. Richter, H. Gao, and Y. Zhu, *ACS nano* **13**, 9082 (2019).
- [5] T. H. Chang, G. M. Cheng, C. J. Li, and Y. Zhu, *Extreme Mechanics Letters* **8**, 177 (2016).
- [6] S. Yin, G. Cheng, T.-H. Chang, G. Richter, Y. Zhu, and H. Gao, *Nature communications* **10**, 2004 (2019).
- [7] T.-H. Chang and Y. Zhu, *Applied Physics Letters* **103**, 263114 (2013).
- [8] The authors acknowledge funding from the National Science Foundation (NSF) under Award No. CMMI-1762511, and the use of the Analytical Instrumentation Facility (AIF) at North Carolina State University (NSF Award No. ECCS-1542015).